

Study of the $C^{14}(p,n)N^{14}$ and $C^{14}(\alpha,n)O^{17}$ Reactions*

RICHARD M. SANDERS†

University of Wisconsin, Madison, Wisconsin

(Received August 17, 1956)

Targets of 38.7% carbon 14, deposited from a glow discharge in acetylene, were used for the determination of the following threshold energies: $C^{14}(p,n)N^{14}$, 671.5 ± 0.5 kev; $C^{14}(p,n)N^{14*}$, 3149.6 ± 1.1 kev; $C^{14}(\alpha,n)O^{17}$, 2340 ± 3 kev. Corresponding reaction energies are -626.4 ± 0.5 , -2938.3 ± 1.0 , and -1820 ± 2 kev. The latter two thresholds were detected by the counter-ratio technique. The $C^{14}(p,n)N^{14}$ excitation curve was extended to 3.4 Mev, covering a resonance at 2908 ± 4 kev with a natural width of 71 ± 5 kev. Resonance energies agree with previous experimental results but the widths are larger, perhaps due to target thickness errors.

Absolute cross sections are compared with those of $N^{14}(n,p)C^{14}$. Compound nucleus spins and partial widths are calculated. $C^{14}(\alpha,n)O^{17}$ resonances with energies and natural widths of 2553 ± 4 , 1.6 ± 1 ; 2642 ± 3 , 10 ± 1 ; $(2798 \pm 11, 22 \pm 10)?$; 3335 ± 15 , 100 ± 20 ; and 3508 ± 4 , 54 ± 3 kev were observed. The 0° differential cross section at 2642 kev is 31 mb/sterad $\pm 60\%$. An angular distribution taken at this resonance leads to a total cross section of 300 mb and a compound-nucleus spin of either 1^- or 3^- . A method is presented for evaluating resonance width, height, and area to find target thickness and natural width.

INTRODUCTION

THE recent availability of carbon 14 in large concentrations has made possible the precision determination of the weak (p,n) and (α,n) thresholds in solid targets of that isotope, thus providing new links in the chain of reactions upon whose energies are based tables of atomic masses.¹⁻⁴ The present work also includes a check on previous observations of the excitation curve for the $C^{14}(p,n)N^{14}$ reaction by the Massachusetts Institute of Technology group⁵ and the Chalk River group,⁶ and a comparison of absolute cross sections with those of the inverse reaction.⁷ An excitation curve for the $C^{14}(\alpha,n)O^{17}$ reaction provides information on five levels in the compound nucleus oxygen 18, in an energy range previously unexplored.

APPARATUS AND METHODS

Beam

The energy of protons or alpha particles from the Wisconsin electrostatic generator⁸ was determined by an electrostatic analyzer⁹ with a resolution of 0.04 to 0.16%, which was calibrated with the ${}^7Li(p,n)Be^7$ threshold, 1881.1 ± 0.5 kev.¹⁰ First-order relativistic corrections¹¹ were applied to obtain the particle energy. The calibration constant was observed to shift system-

atically during the course of a day's operation by an amount of the order of 0.1%. This type of shift, presumably due to temperature change, has been observed before by Taschek *et al.*¹² It has been taken into account in computing errors on the thresholds reported here.

Targets

Targets of C^{14} were prepared according to the techniques of Douglas¹³ by running a high-frequency discharge in acetylene at a pressure of about 0.7 mm Hg between electrodes containing the 10-mil tungsten target backings spaced 1 cm apart. The acetylene was converted, by the method of Monat *et al.*,¹⁴ from barium carbonate enriched to 38.7% C^{14} supplied by Oak Ridge National Laboratory. Targets thus prepared consisted of a greenish-brown deposit of unknown composition which turned dark brown upon heating in air to $400^\circ C$ and black upon bombardment. The black residue was assumed to be carbon of the same isotopic constitution as the barium carbonate.

In order to avoid errors in energy measurement due to the accumulation of a C^{12} layer on the C^{14} targets, three precautions were taken. First, the target chamber was constructed free of organic materials and isolated from the rest of the vacuum system by means of a cold trap of the type described by Miller.¹⁵ Second, the target was held at 100° – $200^\circ C$ by a jet of hot air during

* Work supported in part by the U. S. Atomic Energy Commission and the Wisconsin Alumni Research Foundation.

† Now at Remington Rand Univac, St. Paul, Minnesota.

¹ J. E. Drummond, Phys. Rev. **97**, 1004 (1955).

² Li, Whaling, Fowler, and Lauritsen, Phys. Rev. **83**, 512 (1951).

³ C. W. Li, Phys. Rev. **88**, 1038 (1952).

⁴ A. H. Wapstra, Physica **21**, 367 (1955).

⁵ Roseborough, McCue, Preston, and Goodman, Phys. Rev. **83**, 1133 (1951).

⁶ Bartholomew, Brown, Gove, Litherland, and Paul, Can. J. Phys. **33**, 441 (1955).

⁷ C. H. Johnson and H. H. Barschall, Phys. Rev. **80**, 818 (1950).

⁸ Herb, Turner, Hudson, and Warren, Phys. Rev. **58**, 579 (1940).

⁹ Warren, Powell, and Herb, Rev. Sci. Instr. **18**, 559 (1947).

¹⁰ Jones, Douglas, McEllistrem, and Richards, Phys. Rev. **94**, 947 (1954).

¹¹ Herb, Snowdon, and Sala, Phys. Rev. **75**, 246 (1949).

TABLE I. Thresholds and reaction energies.

Reaction	E_t , kev	Q , kev
$C^{14}(p,n)N^{14}$	671.5 ± 0.5	-626.4 ± 0.5
$C^{14}(p,n)N^{14*}$	3149.6 ± 1.1	-2938.3 ± 1.0
$C^{14}(\alpha,n)O^{17}$	2340 ± 3	-1820 ± 2

¹² Taschek, Argo, Hemmendinger, and Jarvis, Phys. Rev. **76**, 325 (1949).

¹³ Douglas, Gasten, and Mukerji, Can. J. Phys. (to be published).

¹⁴ Monat, Robbins, and Ronzio, U. S. Atomic Energy Commission Report AECU-672 (unpublished).

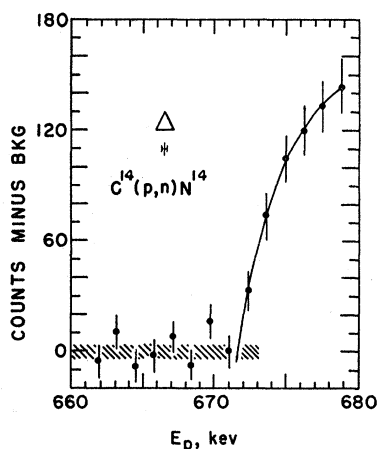
¹⁵ G. H. Miller, Rev. Sci. Instr. **24**, 549 (1953).

bombardment. Third, a fresh target, or a fresh spot on the target, was used for each of the final threshold runs. No correction for target contamination was applied to any of the thresholds.

Detectors

For the $C^{14}(\alpha,n)O^{17}$ excitation curve, the neutron detector was a National Radiac Company Type NBS-1 boron-loaded ZnS(Ag) scintillator on a 6467 photomultiplier tube. The moderator was a $3\frac{7}{8}$ -in. diameter paraffin cylinder $6\frac{1}{4}$ in. long with a central $1\frac{1}{2}$ -in. diameter hole $2\frac{1}{4}$ in. deep in one end for the phototube-scintillator assembly. The dependence of its efficiency upon neutron energy was not known. The detector for the $C^{14}(p,n)N^{14}$ excitation curve and ground-state threshold and the $C^{14}(\alpha,n)O^{17}$ angular distribution was the "long counter,"¹⁶ located $2\frac{1}{2}$ in. from the target for the former and 1 meter from the target for the latter.

FIG. 1. $C^{14}(p,n)N^{14}$ ground-state threshold. The triangle represents beam energy distribution, the energy interval beneath it the uncertainty in the energy scale calibration, and the shaded area the background observed below threshold.



For the $C^{14}(p,n)N^{14}$ excited-state and $C^{14}(\alpha,n)O^{17}$ ground-state thresholds, the ratio-counter technique¹⁷ was used. This technique employs two BF_3 proportional counters: one the standard long counter located a foot or so from the target; the other a shorter counter with a small moderator (the "slow counter") which has enhanced sensitivity to the low-energy threshold neutrons and is located as close to the target as possible. A rise in the ratio of counts in the slow counter to counts in the long counter indicates an excited-state threshold. This arrangement was modified by the insertion of paraffin plugs in the holes in the face of the long-counter moderator to reduce its sensitivity to slow neutrons and the addition of a $1\frac{1}{2}$ -in. wall of borax in front of the long counter to prevent fast neutrons from being moderated in the long counter and diffusing back into the slow counter. These modifications result in a greater change

¹⁶ A. O. Hanson and J. L. McKibben, Phys. Rev. **72**, 673 (1947).

¹⁷ K. I. Greisen, U. S. Atomic Energy Commission Report MDDC-1545, 1945 (unpublished), and T. W. Bonner and C. F. Cook, Phys. Rev. **96**, 122 (1954).

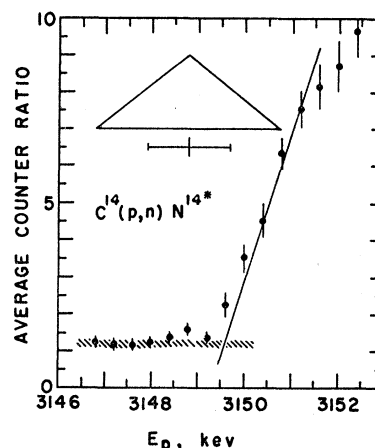


FIG. 2. $C^{14}(p,n)N^{14}$ excited-state threshold. See Fig. 1 for meaning of symbols.

in the ratio at a threshold. The ratio technique was used for the $C^{14}(\alpha,n)O^{17}$ ground-state threshold because of the weak yield, which was not much stronger than the background from the $C^{13}(\alpha,n)O^{16}$ reaction in the target.

RESULTS AND DISCUSSION

Thresholds

Table I contains the results for the three threshold measurements. Reaction energies are calculated from the measured thresholds and atomic masses. Figures 1, 2, and 3 show the experimental data. In these figures, the triangle represents beam energy distribution, the energy interval beneath it the uncertainty in the energy scale due to the $Li(p,n)$ threshold calibration and analyzer shifts, and the shaded area the background below threshold. The threshold is taken as the intersection of the background with the smooth curve, which is drawn below, not through, the experimental points near threshold so that the points will form a fillet in the intersection of approximately the dimensions one would expect from the beam energy resolution.

Negative counts in Fig. 1 are due to the manner of correcting for background. Six counts at each of 14 energies between 661 keV and 679 keV are totaled to obtain 14 datum points. The 8 points below 672 keV have about the same counting rate as the background observed with no beam, so the total neutron count at

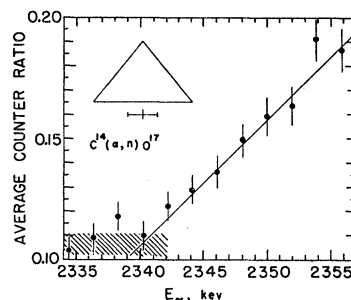


FIG. 3. $C^{14}(\alpha,n)O^{17}$ ground-state threshold. See Fig. 1 for meaning of symbols.

TABLE II. Reactions closing cycles with $N^{14}(\alpha,p)O^{17}$.

Reaction	Q , kev	Reaction	Q , kev	Reaction	Q , kev
$C^{14}(p,n)N^{14}$	-626.4 ± 0.5	$O^{16}(d,\alpha)N^{14}$	3115 ± 2.5^a	$O^{17}(d,\alpha)N^{16}$	9807 ± 12^b
$C^{14}(\alpha,n)O^{17}$	-1820 ± 2	$O^{16}(d,p)O^{17}$	1919 ± 4^a	$N^{14}(d,p)N^{15}$	8614 ± 7^a
Difference:	1193.6 ± 2.1		1196 ± 5		1193 ± 14

^a See reference 19.

^b Pauli, Ahnlund, and Mileikowsky, *Arkiv Fysik* 8, 213 (1954).

each energy is corrected individually for a background consisting of the average counting rate of these 8 points.

The thresholds in Figs. 2 and 3 were run with the ratio counters. The ratio is computed for each count, then all the ratios at the same energy are averaged. Points of Fig. 2 represent the average of 2 ratios, points of Fig. 3, 8. An attempt was made with the ratio counters to observe the 3.45-Mev threshold due to the $C^{14}(\alpha,n)O^{17}$ reaction going to the first excited state (870 kev) in O^{17} , but no statistically significant change in the ratio was detected from 3.4 to 3.6 Mev in a single run, and generator trouble prevented a second run at this energy.

Shoupp *et al.*¹⁸ found a $C^{14}(p,n)N^{14}$ threshold which, when adjusted to the current $Li(p,n)$ threshold, becomes 663 ± 9 kev. The present result, 671.5 ± 0.5 kev, corresponding to a Q of -626.4 ± 0.5 kev, is in better agreement with Van Patter and Whaling's average¹⁹ of experimental Q values for the inverse reaction, 624 ± 4 kev. No previous measurements of the $C^{14}(\alpha,n)O^{17}$ threshold have been reported. The difference between ground and excited state Q values in $C^{14}(p,n)N^{14}$, 2311.9 ± 1.2 kev, agrees well with the excitation energy of 2313 ± 5 kev in N^{14} found by Bockelman *et al.*²⁰ in inelastic proton scattering on N^{14} .

The reaction $N^{14}(\alpha,p)O^{17}$ closes a cycle with the two ground-state thresholds of the present work; unfortunately no precise measurement has been reported of the Q value of this reaction or its inverse. It also closes cycles with two other pairs of reactions, whose energies are given in Table II as a check on the present results. Another check is to compute the reaction energies from a compilation of atomic masses based on a least-squares evaluation of nuclear reaction energies (including beta decay) and mass-spectroscopic doublets. The results, using three such compilations, are given in Table III.

TABLE III. Reaction energies in kev calculated from mass tables.

Reaction	Present data	Drummond ^a	Li <i>et al.</i> ^b	Wapstra ^c
$C^{14}(p,n)N^{14}$	-626.4 ± 0.5	-626.4 ± 3.3	-627 ± 15	-628 ± 5
$C^{14}(\alpha,n)O^{17}$	-1820 ± 2	-1810 ± 6	-1825 ± 18	-1825 ± 7

^a See reference 1.

^b See reference 2.

^c See reference 4.

¹⁸ Shoupp, Jennings, and Sun, *Phys. Rev.* 75, 1 (1949).

¹⁹ D. M. Van Patter and W. Whaling, *Revs. Modern Phys.* 26, 402 (1954).

²⁰ Bockelman, Browne, Buechner, and Sperduto, *Phys. Rev.* 92, 665 (1953).

An independent calculation of the neutron-proton mass difference is possible using the $C^{14}(p,n)N^{14}$ Q value and the C^{14} beta end point. The latter has been variously reported at 155 ± 1 kev,^{21,22} 156.3 ± 1.0 kev,²³ 157.5 ± 5 kev,²⁴ and 158.0 ± 0.5 kev,²⁵ yielding, with the present result, $n-p$ mass differences from 781.4 to 784.4 kev. This approach to the $n-p$ mass difference apparently remains inferior to that using the $T^3(p,n)He^3$ reaction energy¹⁹ and the T^3 beta end point.²⁶ The latter is only 18 kev and subject to smaller absolute errors than the C^{14} end point. The $n-p$ mass difference computed thus is 782 ± 1 kev.

$C^{14}(p,n)N^{14}$ Excitation Curve

The excitation curve for the $C^{14}(p,n)N^{14}$ reaction (Fig. 4) was investigated from 0.67 to 3.4 Mev with a target about 12 kev thick at 1.16 Mev. From the data plotted in Fig. 4 and from two additional runs on the 1.16-Mev resonance are derived the first 9 columns of Table IV. Results of other investigators are presented for comparison.

Target thickness and the natural width given in Table IV for the 1.16-Mev resonance are the results of a method of treating the measurements of height, width, and area of a resonance peak in the excitation curve (see Appendix). The method neglects the effect of finite beam energy resolution and is most useful when target thickness and natural width are of the same order of magnitude. It applies to the treatment of data with a single target, and proves internally consistent when results with targets of different thickness are compared. The target thickness so determined is then adjusted for change of stopping power with energy. The natural widths of the other resonances, whose areas are not measured, are inferred from target thickness and observed width. Because of the asymmetry of the 1.16-Mev resonance, attributed to target nonuniformity, the width and area of the low-energy side only are measured, and the corresponding quantities for the full resonance are taken as twice these values. The same asymmetry is evident in the 2.55- and 2.64-Mev resonances in the $C^{14}(\alpha,n)O^{17}$ excitation curve, discussed below. When the

²¹ S. D. Warsaw, *Phys. Rev.* 80, 111 (1950).

²² H. H. Forster and A. Oswald, *Phys. Rev.* 96, 1030 (1954).

²³ Cook, Langer, and Price, *Phys. Rev.* 74, 548 (1948).

²⁴ Angus, Cockcroft, and Curran, *Phil. Mag.* 40, 522 (1949).

²⁵ Pohm, Waddell, Powers, and Jensen, *Phys. Rev.* 97, 432 (1956), and A. V. Pohm (private communication).

²⁶ R. W. King, *Revs. Modern Phys.* 26, 327 (1954).

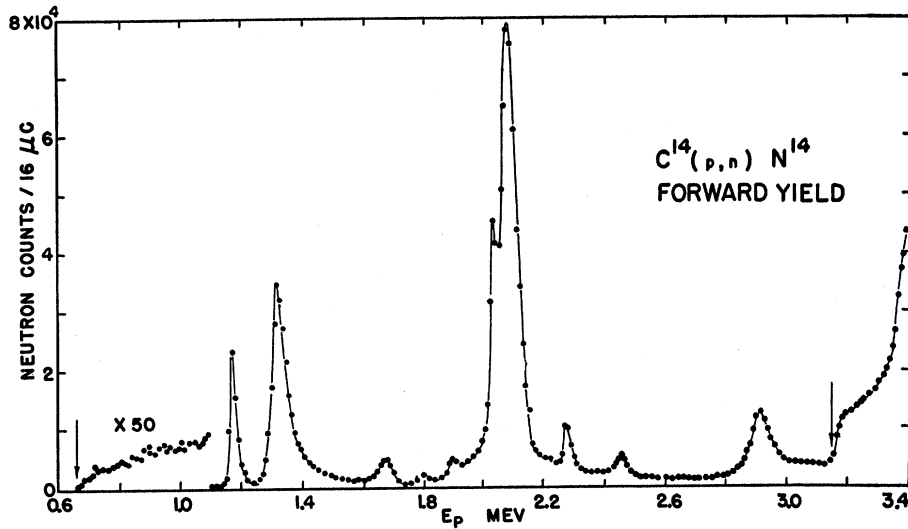


FIG. 4. C¹⁴(p, n)N¹⁴ excitation curve. Arrows indicate neutron thresholds. Approximately half of the off-resonance datum points have been omitted to avoid congestion.

same method is applied to these resonances for the determination of target thickness and natural width, the same target appears significantly thinner at the narrow resonance than at the wide one. This is taken as an indication that the effect of target nonuniformity is not entirely suppressed by restricting attention to the low-energy side of a resonance, and that there is a tendency for the method to give too low a result for the thickness of a nonuniform target if it is of the order of or greater than natural width. If the result for target thickness is too low, then the natural widths of the remaining C¹⁴(p, n)N¹⁴ resonances are subject to an error due to the manner in which their determination depends on target

thickness. This error is not included in the uncertainties in Γ given in Table IV, but is in the right direction to explain the fact that the natural widths in the present work are predominantly larger than the MIT values.

The absolute differential cross sections are based on a comparison with the long counter of a Ra-Be standard neutron source with the 1.16-Mev yield. The Chalk River angular distributions⁶ are used to convert differential to total cross sections. Target density was determined by microbalance weighing to an accuracy of 15%. Other uncertainties are: long-counter efficiency, 15%²⁷; natural width at 1.16 Mev, 20%; statistics, 5%; Ra-Be source, 5%. The over-all uncertainty in absolute

TABLE IV. Comparison of data on C¹⁴(p, n)N¹⁴ resonances. E_x =excitation energy in compound nucleus; E_0 =resonance energy in laboratory system; Γ =natural width in laboratory system; $d\sigma_0/d\omega$ =resonant differential cross section at 0° in the center-of-mass system; σ_0 =resonant total cross section; Γ_n , Γ_p , and Γ_α =neutron, proton, and alpha widths, respectively, in the laboratory system.

$E_x(N^{14})^d$ Mev	Present data							Johnson and Barschall ^a			M. I. T. ^b			Chalk river ^c						
	E_0 keV	Γ keV	$d\sigma_0/d\omega$ mb/sterad	σ_0 mb	J	Γ_n keV	Γ_p keV	Γ_α keV	E_0^e keV	Γ^f keV	σ_0^g mb	E_0^h keV	Γ keV	0° yield ⁱ	E_0 Mev	Γ keV	90° yield ⁱ	J	Γ_n keV	Γ_p keV
11.291	1162±2	6±1	32	400	1/2	<1	>5	0	1170±5	155	1165±2	8±1	42 ^k	1.165	12	22	1/2, (3/2)	1.6	10.4	
11.433	1314±3	54±3	25	315	1/2	44	10	0	1311±7	55	290	1310±3	43±5	25	1.31	41	25	1/2	32.8	8.2
11.765	1670±3	56±3	3.6	45	3/2	55	0.8	0	1664±12	60	36	1664±4	38±10	2.9	1.66	37	4.5	3/2	36.5	0.5
11.875	1788±3	22±2	1.7	21	3/2	22	0.1	0.05				1789±4	18±5	1.3	1.79	24.5	2.5	3/2, 5/2	24.5	0.03
11.965	1884±3	18±2	3.8	48	1/2	17	0.7	0.26		29	1883±4	15±5	2.9	1.88	21.5	7	1/2	21.2	0.3	
12.097	2026±4	27±5	35	330	5/2	24	2.5	0.6				2024±4	18±5	24	2.02	18	35	5/2	17.2	0.8
12.146	2079±4	58±8	59	650	3/2	38	18	2.2	2086±15	70	390	2079±4	55±10	53	2.08	53	61	3/2, 5/2	38.0	15.0
12.326	2271±4	23±3	8.7	73	5/2	22.5	0.4	0.1				2272±4	22±5	~6	2.27	22	5/2	21.7	0.3	
12.493	2450±4	34±4	4.1		3/2 ^l	28	0.3	5.5				2451±10	45±20	~2.4						
12.920	2908±4	71±5	9.7																	

^a Reference 7.
^b Reference 5.
^c Reference 6.
^d The atomic-mass tables of reference 2 are used in computing excitation energies.
^e E_0 of reference 7 + 671 keV.
^f Scaled from Fig. 3 of reference 7.
^g See reference 5 for the method of calculating σ_0 by detailed balancing from the cross sections of reference 7.
^h Based on a Li(p, n) threshold of 1882.2 keV.
ⁱ (25/17) times the "Y max" column of Table II of reference 5.
^j Normalized at 1.31 MeV.
^k Corrected for target thickness, assuming $\Gamma = 7$ keV.
^l Based on $\sigma_{np} = 10$ mb, estimated from reference 7.

²⁷ W. D. Allen, U. S. Atomic Energy Research Establishment Report NP/R 1667, 1955 (unpublished).

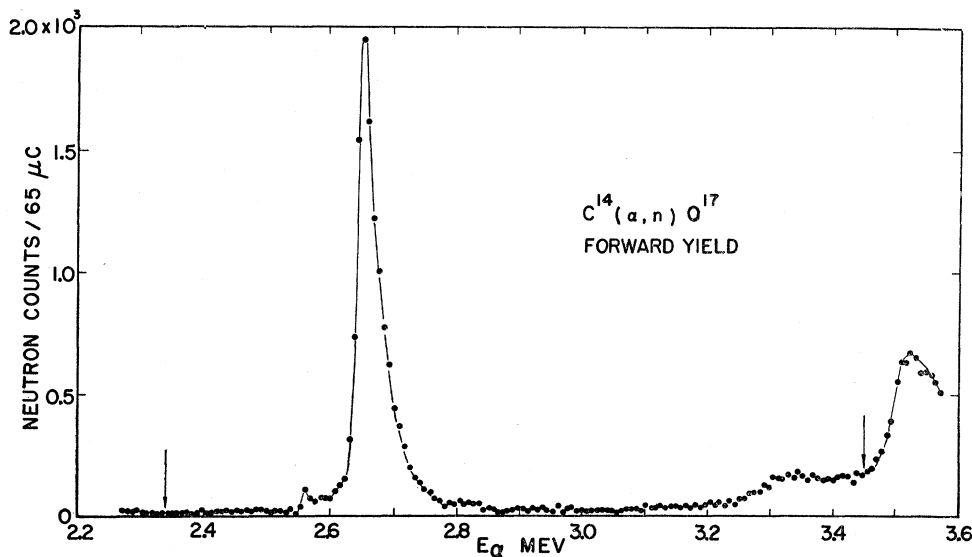


FIG. 5. $C^{14}(\alpha, n)O^{17}$ excitation curve. Arrows indicate neutron thresholds. The threshold at 3.45 Mev was not observed. Background below 2.34 Mev threshold is from $C^{13}(\alpha, n)O^{16}$.

cross sections at 1.16 Mev is the rms total of these or about 30%. At the other resonances, cross sections are determined by a comparison of yields with the 1.16-Mev yield, and they may be subject to an additional error due to energy dependence of the long counter sensitivity to a neutron source (target) only a few inches from the counter.

Spins of the various compound-nucleus levels are found as follows: The Breit-Wigner one-level formula specialized for the $N^{14}(n, n)N^{14}$ reaction at resonance is

$$\sigma_{nn} = \frac{2}{3}\pi\lambda_n^2(2J+1)\Gamma_n^2/\Gamma^2.$$

However, Γ_n/Γ is equal to σ_{nn}/σ_t (σ_t is the total resonant cross section of nitrogen 14 for neutrons of wavelength λ_n). Hence, we have

$$2J+1 = 3\sigma_t^2/2\pi\lambda_n^2\sigma_{nn}.$$

Values of σ_t are taken from the paper of Hinchey *et al.*²⁸ (where they are called S_t). Values of σ_{nn} are the σ_t minus the σ_{np} converted according to the principle of detailed balance from the values of σ_{pn} of the present work, minus the $\sigma_{n\alpha}$ of Johnson and Barschall⁷ increased by 10% to correct for their large neutron energy spread. The nearest half-integer to the solution for J is given in Table IV. The accuracy of these values depends pri-

TABLE V. Resonances in $C^{14}(\alpha, n)O^{17}$. See Table IV for definitions of symbols.

E_n , kev	Γ , kev	$E_x(O^{18})$, Mev
2553 ± 4	1.6 ± 1	8.223
2642 ± 3	10 ± 1	8.293
2798 ± 11^a	22 ± 10	8.414
3335 ± 15	100 ± 20	8.832
3508 ± 4	54 ± 3	8.966

^a The 2798-kev resonance must be regarded as doubtful because of its absence in later data (to be published) on alpha scattering on C^{14} .

²⁸ Hinchey, Stelson, and Preston, Phys. Rev. **86**, 483 (1952).

marily upon the accuracy of the σ_t , which is difficult to estimate. While we are not prepared to rule out any of the possibilities for J given in the Chalk River paper, we can indicate preferred values for all the levels.

Partial widths Γ_n , Γ_p , and Γ_α are the fractions σ_{nn}/σ_t , σ_{np}/σ_t , and $\sigma_{n\alpha}/\sigma_t$, respectively, of the total width Γ . It appears that Γ_α cannot be neglected at the 2.08-Mev resonance, as was done in the Chalk River paper.⁶

$C^{14}(\alpha, n)O^{17}$ Excitation Curve

Figure 5 is the excitation curve for the $C^{14}(\alpha, n)O^{17}$ reaction between 2.3 and 3.6 Mev. Additional data were taken on most of the resonances, yielding the results presented in Table V.

The differential cross section at the 2.64-Mev resonance is 31 mb/sterad at 0° and the total cross section, based on the angular distribution discussed below, 300 mb. The value of the target surface density used in finding the absolute cross section is not, in this case, the result of weighing but depends on the thickness of the same target estimated at 20 kev from both sides of the 1.16-Mev $C^{14}(p, n)N^{14}$ resonance data. Both sides of the resonance are measured because we are concerned here with the total amount of material on the target rather than its effect in widening a resonance or spoiling symmetry. These cross sections are subject to an uncertainty of 50% in target density plus the uncertainties in the $C^{14}(p, n)N^{14}$ cross sections, or about 60% overall.

Angular Distribution of the 2.64-Mev Resonance in $C^{14}(\alpha, n)O^{17}$

The angular distribution of neutrons from the 2.64-Mev resonance in $C^{14}(\alpha, n)O^{17}$ is shown in Fig. 6. The smooth curves are semitheoretical distributions discussed below. The plotted points are the differences, at

resonance, between smooth curves drawn through two observed yields in the vicinity of 2.64 Mev at each angle, one with and one without a 14-in.-long borax-paraffin cone between the target and the long counter 1 meter away, to provide an experimental correction for neutrons scattered into the counter from the floor and walls. These observed yields are transformed into the center-of-mass system and corrected for the slight variation of counter sensitivity with neutron energy. No correction is made for the scattering of neutrons by the target backing and the walls of the target chamber. Neutrons detected in the angular distribution had to pass at various angles through $\frac{1}{32}$ in. of steel plus 0.010 in. of tungsten if emitted in the forward hemisphere or $\frac{1}{16}$ in. of inconel in the back hemisphere.

The absolute cross-section scale is taken from an independent measurement at 0° and contains an uncertainty of 60%. The errors shown on the experimental points are statistical only.

The Wigner limit²⁹ $3\hbar^2/2Ma$ on the reduced neutron width γ_n^2 of this level is 1.3×10^{-9} kev-cm. When compared with reduced widths for various assumed values of neutron angular momentum l_n , this limit implies that $l_n \leq 2$ unless the neutron width Γ_n is of the order of or less than 2% of the observed total width. Moreover, the anisotropic character of the angular distribution cannot arise from a compound nucleus level with a spin J of 0 or if $l_n = 0$. Under these restrictions and the conservation of angular momentum and parity, the remaining possibilities for alpha-particle angular momentum l_α , spin J , parity π , l_n , and outgoing-channel spin s_n are listed in Table VI.

The column headed $W(\theta)$ contains the theoretical angular distributions for each spin possibility calculated with the help of the Chalk River compilation³⁰ of coefficients of Legendre polynomials in the expansion of $W(\theta)$ given by Blatt and Biedenharn.³¹ Since $W(\theta)$ depends upon s_n , only the $J = 1^-$ assignment leads to a unique $W(\theta)$. It is $W(\theta) \propto (3 + \cos^2\theta)$, which makes an acceptable fit with the experimental data. For the other three possibilities, one can choose arbitrary s_n -mixing ratios in

TABLE VI. Possible spin and parity assignments, 2.64-Mev C¹⁴(α, n)O¹⁷ resonance.

l_α	J, π	l_n	s_n	$W(\theta)$
1	1 ⁻	1	2	$(9/10)(3 + \cos^2\theta)$
2	2 ⁺	2	2	$(25/14)(4 - 9 \cos^2\theta + 9 \cos^4\theta)$
			3	$(75/56)(5 - 2 \cos^2\theta - 3 \cos^4\theta)$
3	3 ⁻	1	2	$(21/5)(1 + 2 \cos^2\theta)$
			3	$(21/2)(1 - \cos^2\theta)$
4	4 ⁺	2	2	$(27/56)(13 - 10 \cos^2\theta + 45 \cos^4\theta)$
			3	$(135/28)(1 + 8 \cos^2\theta - 9 \cos^4\theta)$

²⁹ T. Teichman and E. P. Wigner, Phys. Rev. **87**, 123 (1952).

³⁰ Sharp, Kennedy, Sears, and Hoyle, Atomic Energy of Canada Limited Report AECL-97, Chalk River, Ontario, 1953 (unpublished).

³¹ J. M. Blatt and L. C. Biedenharn, Revs. Modern Phys. **24**, 258 (1952).

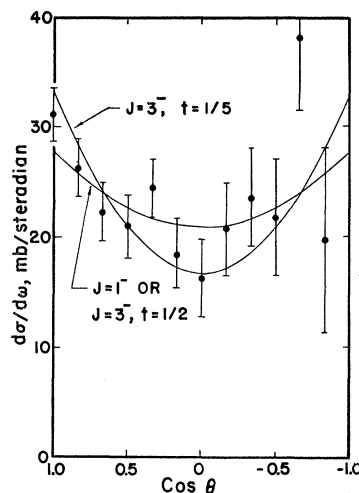


Fig. 6. Odd-parity angular distributions for the 2.64-Mev resonance in C¹⁴(α, n)O¹⁷. Curves are theoretical distributions for given values of the compound-nucleus spin J and the outgoing channel-spin mixing ratio t .

an attempt to find a $W(\theta)$ in reasonable agreement with the data. The $J = 3^-$ assignment conforms readily if t , the ratio of $(s_n = 3) : (s_n = 2)$, is anywhere from 1:2 to 1:5, the former extreme giving a distribution proportional to $3 + \cos^2\theta$ and the latter to $1 + \cos^2\theta$. These are the smooth curves in Fig. 6.

In Fig. 7 the points are weighted averages of the experimental data at supplementary angles and the curves are the unnormalized distributions $W(\theta)$ for the four even-parity cases in Table VI. In the case of $J = 2^+$, it is impossible to get a combination of $s_n = 2$ and $s_n = 3$ with a minimum at $\cos^2\theta = 0$ regardless of the curvature one wishes to accept. In the case of $J = 4^+$, one can fit the data at $\cos^2\theta = 0$ and 1 but only with a combination having a curvature much larger than what the data appear to allow. Evidently the even-parity assignments are excluded by the angular distribution.

The final assignment is the alternate one, $J = 1^-$ or 3^- . In the case of 1^- , the measured total cross section, 300

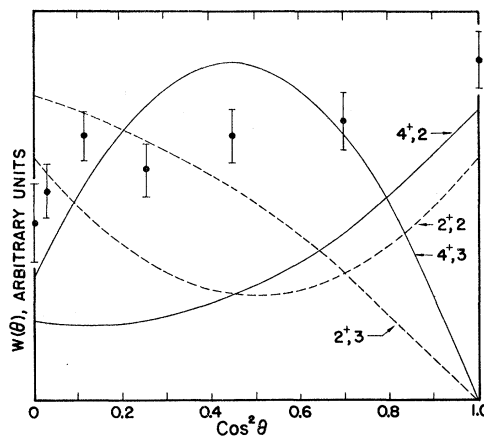


Fig. 7. Even-parity angular distributions for the 2.64-Mev resonance in C¹⁴(α, n)O¹⁷. Curves are theoretical distributions for given values of the compound-nucleus spin J and the outgoing channel spin s_n . Experimental points are weighted averages of data at supplementary angles.

mb, is the maximum $\pi\lambda_\alpha^2(2l_\alpha+1)$ allowed by the Breit-Wigner formula.

ACKNOWLEDGMENTS

I wish to thank Professor H. T. Richards for his suggestion of the project and his valuable guidance; Professor R. G. Herb for assistance in designing the target chamber; Ambuj Mukerji, David Herring, and Rod B. Walton for enlightening discussions of several problems; and Jan Broer, Ren Chiba, and Edward Silverstein for assistance in taking data.

APPENDIX

We shall derive here a method for obtaining target thickness T from the yield curve for a nuclear reaction described by the Breit-Wigner one-level formula for the cross section σ as a function of bombarding energy E in the vicinity of a resonance at energy E_0 with a natural width Γ :

$$\sigma = C[(E - E_0)^2 + \frac{1}{4}\Gamma^2]^{-1}, \quad (1)$$

where C is a constant of proportionality depending on nuclear parameters. The yield $N(E)$ of product particles per incident particle from such a reaction is the integral through successive target layers $d\epsilon$:

$$N(E) = C \int_0^T \frac{n d\epsilon}{(E - \epsilon - E_0)^2 + \frac{1}{4}\Gamma^2}, \quad (2)$$

where n is the number of target nuclei per cm² per energy unit of thickness. (We neglect any spread in beam-energy distribution.) If n is reasonably constant over the target, the result of integration is

$$N(E) = \frac{2Cn}{\Gamma} \tan^{-1} \left[\frac{\frac{1}{2}\Gamma T}{(E - E_0 - T)(E - E_0) + \frac{1}{4}\Gamma^2} \right] \quad (3)$$

and is maximum when E has the value $E_0 + \frac{1}{2}T$. The maximum value N is given by

$$N = (4Cn/\Gamma) \tan^{-1}(T/\Gamma), \quad (4)$$

and the half-maximum points, i.e., $N(E) = \frac{1}{2}N$, occur where

$$E - E_0 = \frac{1}{2}[T \pm (T^2 + \Gamma^2)^{\frac{1}{2}}]. \quad (5)$$

Thus we find that the observed width W at half-maximum is given by

$$W^2 = T^2 + \Gamma^2. \quad (6)$$

We define the area A under a resonance in the yield curve by the following limiting process:

$$A = \lim_{\Delta E \rightarrow 0} [\Delta E \sum_i N(E_i)] = \int N(E) dE, \quad (7)$$

where ΔE is the constant energy interval between points E_i of observation of the yield $N(E_i)$. To find another expression for A , we observe that A depends only upon the total quantity of reacting matter in the target and not upon its stopping power, provided that the target is not thick enough to stop the beam, i.e., not a "thick target" in the usual sense. Hence we can integrate the yield from a very thin target ($T \ll \Gamma$),

$$N(E) = CnT[(E - E_0)^2 + \frac{1}{4}\Gamma^2]^{-1}, \quad (8)$$

to arrive at an expression valid for any T ,

$$A = 2\pi CnT/\Gamma. \quad (9)$$

We can now eliminate C from Eqs. (4) and (9) to show that

$$T/\tan^{-1}(T/\Gamma) = 2A/\pi N \equiv S. \quad (10)$$

From Eqs. (6) and (10) we deduce the relation

$$T/W = \sin(T/S), \quad (11)$$

into which we can substitute values of W and S from the yield curve and solve for T . Then we can find Γ from Eq. (6) and C from either Eq. (4) or (9), and express the resonant cross section σ_0 entirely in terms of measurable quantities in either of two ways:

$$\sigma_0 = N/[n\Gamma \tan^{-1}(T/\Gamma)] = 2A/(\pi nT\Gamma). \quad (12)$$

(The product nT is the target surface density in nuclei/cm², obtainable directly from weighing.)

This method, while derived generally, is most accurate and useful when T and Γ are of the same order of magnitude. It supplements the method of Bernet, Herb, and Parkinson,³² for the treatment of thick- and thin-target data.

³² Bernet, Herb, and Parkinson, Phys. Rev. 54, 398 (1938).